Available online at www.sciencedirect.com
ScienceDirect
Journal of the European Ceramic Society 29 (2009) 913–918
www.elsevier.com/locate/jeurceramsoc

Limits to feature size and resolution in ink jet printing

J. Stringer*, B. Derby

School of Materials, University of Manchester, Grosvenor Street, Manchester M1 7HS, UK

Available online 23 December 2008

Abstract

Ink jet printing is an attractive route for the manufacture of small ceramic parts and MEMS components. The attainable feature size of a component fabricated in this fashion is determined by both the generated droplet size and how the droplet interacts with the substrate. Here we present a study of the impingement and coalescence of drops to form beads, and linear deposits after a subsequent phase change. Experimentally, it is found that there is a minimum width of linear deposit produced in this way that is dependent upon droplet size and the surface energy interaction between droplet and substrate. A simple geometric model is presented that can accurately predict both the onset of limitation with changing droplet separation and the width of the deposit at a given droplet separation. A bulging instability is also found at small droplet separation that is explained in terms of competing pressure-driven axial flow and spreading flow driven by capillarity. The bulging of deposited nanoparticulate ink was found to agree qualitatively with previous observations, with the bulging being reduced with increasing print-head traverse velocity. The bulging of deposited solution-based ink did not agree with previous observations; this was explained in terms of evaporation of solvent as the instability was formed.

Keywords: Ink jet printing; Particle suspension; Solution precursor; MEMS

1. Introduction

Ink jet printing is a solid freeform fabrication technique that shows potential for use in fields such as ceramic part manufacture,[1] MEMS[2] and biomaterials.[3] Ink jet printing is a non-contact printing technique that can deposit droplets of a variety of material-laden inks at predetermined locations on a substrate. By in turn depositing droplets that coalesce into lines, lines that coalesce into sheets and overprinting of sheets, three-dimensional objects can be made. To control the feature size obtained with this process, an understanding of how liquid droplets coalesce into patterns as a function of fluid properties, substrate properties and machine parameters is required.

The deposition mechanism of a discrete droplet can be separated into two stages: an impact-driven stage in which the impact kinetic energy is dissipated, and a surface energy driven stage where the droplet will spread to a diameter dependent upon the surface energy interactions between the ink and the substrate. A solid deposit is formed by the phase change of the ink from a liquid to a solid (e.g. gelation, solidification, evaporation). The size of deposit obtained will either be dependent upon the impact-driven stage if the phase change from liquid to solid is fast (e.g. solidification),[4] or on the surface energy driven stage if the phase change is slower (e.g. evaporation). If gravitational forces are negligible, a liquid droplet deposited on a substrate will equilibrate to a spherical cap with a contact angle, θ, so as to minimise the energy state of the droplet. The value of θ that corresponds to this energy minimum is defined by the Young–Dupre equation (Eq. (1)):

$$\cos\,\theta = \frac{\sigma_{SV} - \sigma_{LS}}{\sigma} \tag{1}$$

where σ_{SV} is the interfacial energy between substrate and air, σ_{LS} is the interfacial energy between droplet and substrate and σ is the interfacial energy between droplet and air. Assuming a spherical cap geometry and conservation of volume between droplet and spherical cap, the extent of droplet spreading upon the substrate so as to minimise surface energy can be calculated (Eq. (2)):

$$\beta_{eqm} = \frac{d}{d_{eqm}} = \sqrt[3]{\frac{8}{\tan(\theta/2)(3 + \tan^2(\theta/2))}} \tag{2}$$

where β_{eqm} is the ratio of the initial droplet diameter, d, to the diameter of the droplet on the substrate, d_{eqm}. The Bond number ($Bo = \rho g d^2/\sigma$, where ρ is the ink density and g is the acceleration due to gravity) indicates the relative influence of surface and gravitational forces. For typical parameters found with ink

* Corresponding author. Tel.: +44 161 306 3583; fax: +44 161 306 8877.
E-mail address: jonathan.stringer@manchester.ac.uk (J. Stringer).

0955-2219/$ – see front matter © 2008 Published by Elsevier Ltd.
doi:10.1016/j.jeurceramsoc.2008.07.016

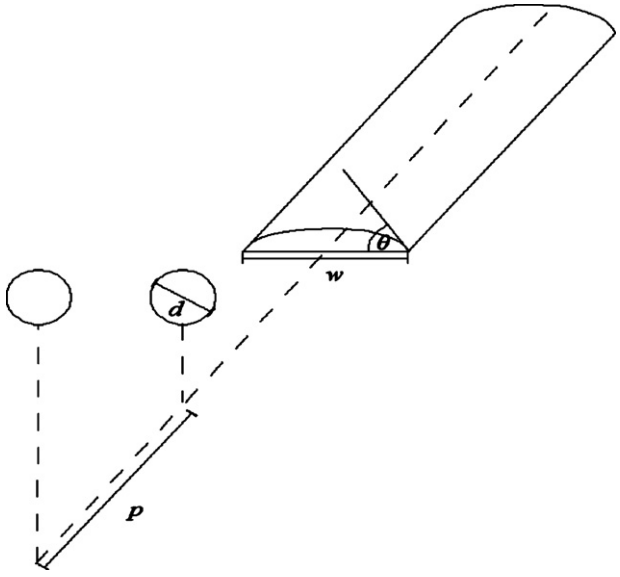

Fig. 1. Diagram of model for predicting bead width from a train of droplets.

Table 1
Fluid properties of the different inks used in this study.

	η/mPa s	σ/mJ m^{-2}
Nanoparticle ink	14.4	31
Organometallic ink	4.14	28

jet printing, the Bond number is approximately 10^{-2} to 10^{-3}, showing that surface forces are dominant and the spherical cap assumption above is valid.

Material-laden inks will often show a contact angle hysteresis due to solid material segregating to the contact line and pinning it.[5] This means that the shape that the ink forms on the substrate at phase change will be the same as the shape of the final deposit. Thus, Eq. (2) will also predict the size of the final deposit on a substrate. Using the same conservation of volume and surface energy balance assumptions as before, a model can be derived for a train of droplets that coalesce to form a liquid bead with a circular segment cross-section (Fig. 1). This model can be made dimensionless with respect to both d and θ to obtain the following universal relationship:

$$\frac{w}{\beta_{\mathrm{eqm}} d} = \sqrt{\frac{2\pi d}{3p\beta_{\mathrm{eqm}}^2((\theta/\sin^2\theta) - (\cos\theta/\sin\theta))}} \quad (3)$$

where w is the width of the formed bead and p is the spacing between deposited droplets. In the presence of contact line pinning, the smallest stable bead size, $w_{\min}$, possible will be the diameter of a single droplet at equilibrium on a substrate. A threshold, $p_{\max}$, above which liquid beads will not have parallel contact lines can be derived from Eq. (3):

$$p_{\max} = \sqrt{\frac{2\pi d}{3\beta_{\mathrm{eqm}}^2((\theta/\sin^2\theta) - (\cos\theta/\sin\theta))}} \quad (4)$$

The largest stable bead size, $w_{\max}$, is a more complex situation, influenced by the fluid properties of the ink, the rate of phase change and the flow rate of ink into the bead. For solidifying systems, it has been found that a bulging of the bead occurs when the apparent contact angle formed upon solidification of the liquid ridge exceeds 90°. The stability of solidifying beads is therefore strongly influenced by the temperature difference between droplet and substrate.[4] With evaporating systems, a series of regular bulges connected by ridges of width equal to d_{eqm} has been observed.[6] This has been explained in terms of two competing flows within the bead; an outward spreading flow due to capillarity and an axial flow driven by pressure differences inherent within the deposited bead. The largest stable bead size that can be obtained under these conditions, $w_{\max}$, should increase with decreasing θ, decreasing σ, increasing ink viscosity, η, and increasing print head traverse velocity, U_t. The work assumed that the phase change of the ink has negligible impact upon the formation of the instability besides pinning the contact line, which is likely to be invalid in faster evaporating systems as evaporation will increase η and alter σ.

2. Experimental procedure

The inks used in this study were a commercial silver nanoparticle ink (Inkjet Silver Conductor AG-IJ-G-100-S1, CABOT-PED, Albuquerque, NM, USA) and an organometallic salt dissolved in xylene synthesised in-house. Preparation details for the synthesis of the organometallic solution have been published previously.[7] The substrates used in this study were glass (microscope slides, BDH, Poole, Dorset, UK), polyimide film (Kapton^{TM}, DuPont, Wilmington, DE, USA) and silicone rubber (Goodfellow Cambridge Ltd., Huntingdon, Cambs., UK). The equilibrium contact angle, θ, of each ink/substrate combination was measured using a CCD camera and image analysis software (FTA 200, Camtel, Royston, UK). Both inks used have previously been characterised with regards to surface tension

Table 2
Comparison of measured and calculated β_{eqm} from measured θ values.

Ink	Substrate	θ/°	β_{eqm} (calculated)	β_{eqm} (measured)
Nanoparticle	Glass	15.5 ± 2.2	2.69 ± 0.14	2.60 ± 0.06
Nanoparticle	Polyimide	45.2 ± 0.8	1.82 ± 0.03	1.85 ± 0.08
Nanoparticle	Silicone	63.4 ± 1.1	1.56 ± 0.02	1.58 ± 0.04
Organometallic	Glass	22.0 ± 1.4	2.38 ± 0.03	2.37 ± 0.05
Organometallic	Polyimide	10.8 ± 2.4	3.04 ± 0.26	2.99 ± 0.10
Organometallic	Silicone	47.0 ± 1.3	1.79 ± 0.02	1.81 ± 0.04

and viscosity, either in previous publications[7] or on data sheets supplied with the ink. This data is summarised in Table 1.

Printing of samples was carried out using a JetLab printing platform (MicroFab Inc., Plano, TX, USA) that consists of a piezoelectric squeeze mode print head situated above a programmable x–y platform. The print heads used in this study had a nozzle diameter of 50 μm (MJ-SF-01-50, MicroFab, as above). Droplet diameter measurements were conducted by ejecting a known number of droplets into a vial containing an appropriate solvent. The mass change of this vial was compared with an identical reference vial filled with the same solvent and a mass balance used to calculated the diameter of an individual droplet, assuming a spherical droplet and known density values. All substrates were cleaned with acetone before deposition of droplets. The two variables investigated using this apparatus were p and U_t.

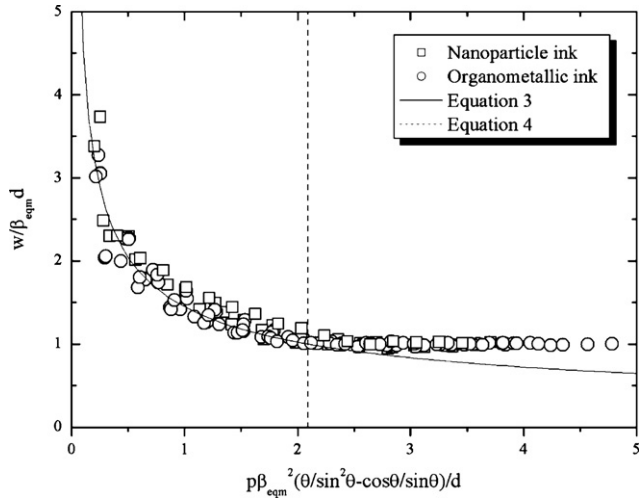

Fig. 3. Comparison of measured w with varying p for both organometallic and nanoparticulate ink with Eqs. (3) and (4).

3. Results and discussion

The size of an individual droplet was measured as described above and was found in both cases to be slightly greater than the nozzle diameter ($d = 61$ μm for the nanoparticulate ink, $d = 56$ μm for the organometallic ink). This shows that the primary limitation on droplet size is the nozzle diameter, with the nozzle diameter limited by the viscous dissipation as fluid is forced through it.[8]

The deposit left by individual droplets of both inks on each substrate were measured and compared with the diameter as calculated using Eq. (2) (Table 2). In all cases, good agreement was shown between experimental and calculated diameters, showing that gravitational effects are negligible and that contact line pinning takes place due to segregation of the solid component of the ink.

The impact velocity of both droplets were similar (2.3 ms^{-1} for the organometallic ink and 2.8 ms^{-1} for the nanoparticle ink), which gave an impact kinetic energy similar to the initial surface energy of the droplet. Further experiments were

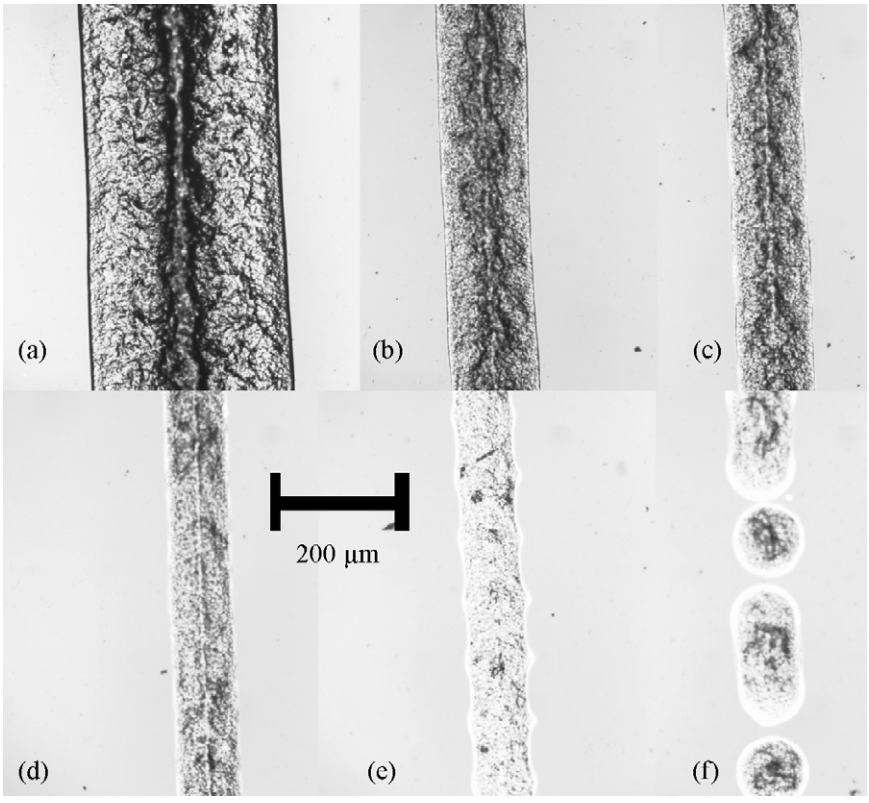

Fig. 2. A typical series of deposits formed from liquid beads of organometallic ink on a glass substrate. p varies from 10 μm to 160 μm in 30 μm intervals from a to f.

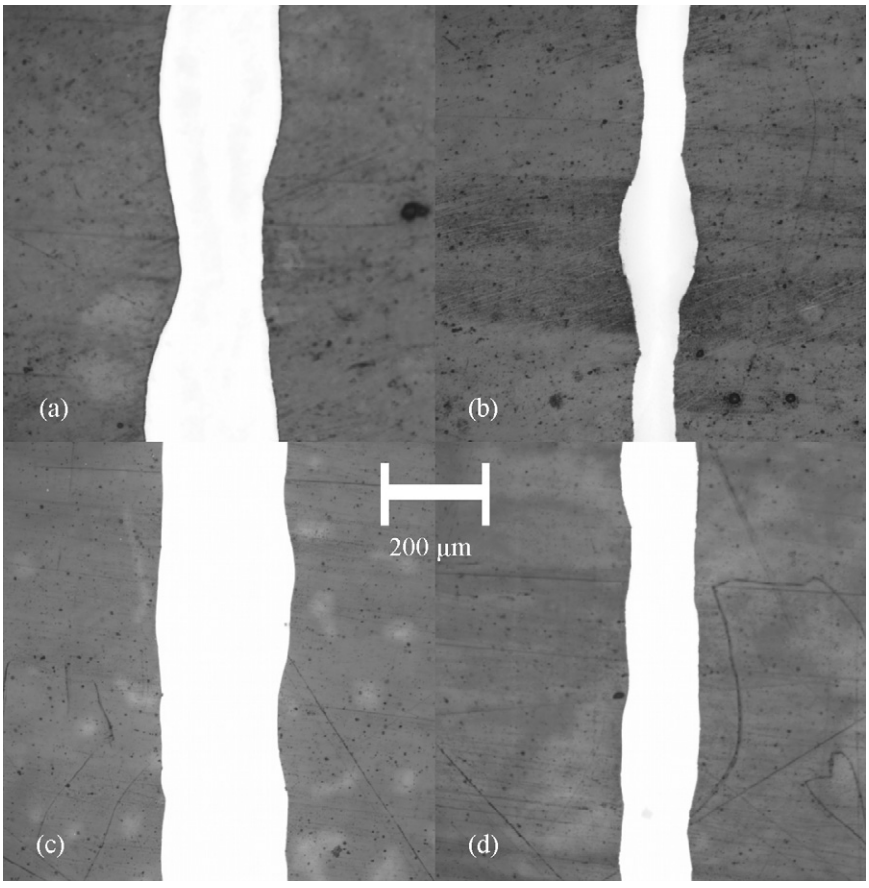

Fig. 4. Deposits of nanoparticulate ink on polyimide with $U_t = 0.01\ ms^{-1}$ for (a) and (b) and $U_t = 0.1\ ms^{-1}$ for (c) and (d). $p = 20\ \mu m$ for (a) and (c) and $p = 80\ \mu m$ for (b) and (d).

carried out with the organometallic ink at a higher impact velocity ($4.2\ ms^{-1}$), and no difference was found in the spreading behaviour. This shows that the impact-driven spreading seems to have no influence on the deposit size.

The deposits formed from beads of coalesced droplets (Fig. 2) were measured and compared with Eqs. (3) and (4) (Fig. 3). For both the nanoparticulate and organometallic inks, observation agreed well with predictions from Eq. (2). The threshold of track stability predicted by Eq. (3) also agreed well with experimental data, as shown by the measurements following a straight line beyond this point. The points beyond the threshold predicted by Eq. (4) initially showed a curvature of the contact line due to contact angle hysteresis (Fig. 2e) as p was increased. With further increase in p, the droplets no longer coalesce into a continuous track, instead forming a series of discrete droplet depositions (Fig. 2f).

In all cases a region could be identified below the threshold defined by Eq. (4) in which the relationship defined by Eq. (3) was obeyed. This shows that it is possible to form a bead, and therefore deposit, with parallel contact lines if θ and d are known, and p adjusted accordingly. The size of this region was found to decrease with increasing θ, signifying that alteration of θ as a means of controlling feature size has to be performed carefully if a deposit with parallel contact lines is to be achieved.

At low droplet spacing, a variety of bulging instabilities were observed (Figs. 4 and 5). With the nanoparticle ink (Fig. 4), these bulges appeared similar to those observed by Duineveld,[6] with the connecting ridge between bulges approximating to d_{eqm} in all but the shortest droplet spacing. The occurrence of these instabilities was noticeably reduced with an increase in U_t, suggesting that the theory proposed by Duineveld[6] is valid and that the evaporation of solvent does not play a significant role in the formation of these instabilities.

The deposits formed by the organometallic ink also showed bulging instabilities at low droplet spacing (Fig. 5), but the connecting ridges were significantly greater than d_{eqm} and their presence was not reduced by an increase in U_t. The increased width of these ridges could be indicative of the significance of evaporation within the bead formation process. Initially, the axial flow is dominant over the capillary flow within the ridge and a bulge will form. As the process proceeds, evaporation increases the viscosity of the fluid within the bead and the capillary flow will become dominant, causing the ridge to spread outwards.

The presence of bulges at both high and low U_t is most probably due to evaporation counteracting the increased flow of fluid into the ridge. An increased U_t will increase the frequency of droplet deposition and reduce the amount of time between each deposition for a given p. The beads produced at low U_t will therefore have more time for evaporation between droplet depositions and the viscosity of the fluid in the ridge will be increased, encouraging capillary flow.

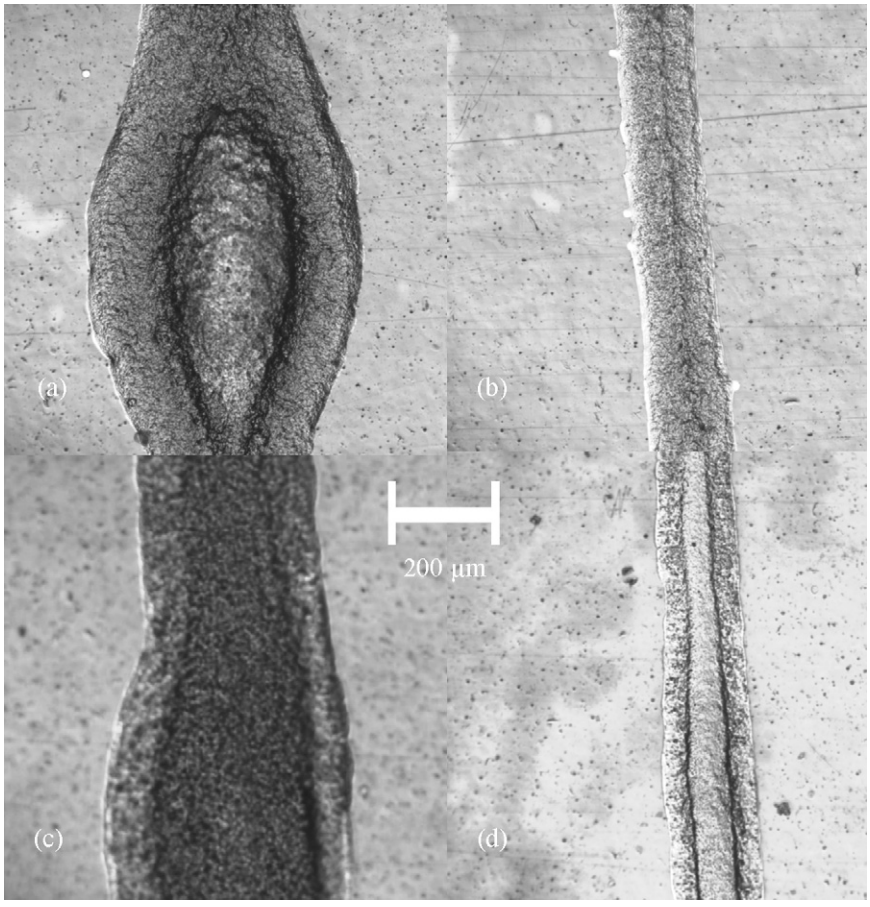

Fig. 5. Deposits of organometallic ink on polyimide with $U_t = 0.01\ ms^{-1}$ for (a) and (b) and $U_t = 0.1\ ms^{-1}$ for (c) and (d). $p = 20\ \mu m$ for (a) and (c) and $p = 80\ \mu m$ for (b) and (d).

4. Conclusion

The formation of deposits by ink jet printing a series of coalescing droplets of material-laden (nanoparticle suspension and solution) ink was investigated. It was found that deposits with parallel contact lines could be formed within certain ranges of droplet separation, p. The track width, w, could be predicted on a variety of substrates with different contact angle, θ, using a simple geometric model, showing that gravitational forces were negligible. The maximum value of p was predicted using the same model and experimental observations showed good agreement. The relationships described by Eqs. (2) and (3) were closely matched by experimental behaviour of both nanoparticulate and solution inks, meaning that such behaviour should be universal for all fluids that exhibit contact angle hysteresis, such as ceramic suspensions and salt solutions.

At low values of p, a series of bulging instabilities was observed, which were explained in terms of the competing axial flow through the liquid bead and the spreading flow due to capillarity. Results using nanoparticulate ink showed qualitative agreement with previous observed behaviour. Results using organometallic ink also showed bulging, but the width of the connecting ridge between each bulge was significantly larger than the nanoparticulate ink. This was believed to be due to the increased influence of evaporation on the flow within the liquid bead. Again, this behaviour should be universal for fluids that exhibit contact angle hysteresis, with the nature of the bulging dependent upon the evaporation rate of the carrier solvent.

Acknowledgements

The authors would like to acknowledge Steven Yeates and Veronica Sanchez Romaguera (Department of Chemistry, University of Manchester, UK) for use of the CABOT-PED nanoparticulate ink. This work was funded by the Office of Naval Research through grant N00014-03-1-0930.

References

1. Ainsley, C. *et al.*, Freeform fabrication by controlled deposition of powder filled melts. *J. Mater. Sci.*, 2002, **37**(15), 3155–3161.
2. Fuller, S. B. *et al.*, Ink-jet printed nanoparticle microelectromechanical systems. *J. MEMS*, 2002, **11**(1), 54–60.
3. Sachlos, E. *et al.*, Novel collagen scaffolds with predefined internal morphology made by solid freeform fabrication. *Biomaterials*, 2003, **24**(8), 1487–1497.
4. Schiaffino, S. and Sonin, A. A., Formation and stability of liquid and molten beads on a solid surface. *J. Fluid Mech.*, 1997, **343**, 95–110.

5. Deegan, R. D. *et al.*, Contact line deposits in an evaporating drop. *Phys. Rev. E*, 2000, **62**(1), 756–765.
6. Duineveld, P. C., The stability of ink-jet printed lines of a liquid with zero receding contact angle on a homogeneous substrate. *J. Fluid Mech.*, 2003, **477**, 175–200.
7. Dearden, A. L. *et al.*, A low curing temperature silver ink for use in ink-jet printing and subsequent production of conductive tracks. *Macromol. Rapid Commun.*, 2005, **26**, 315–318.
8. Fromm, J. E., Numerical calculation of the fluid dynamics of drop-on-demand jets. *IBM J. Res. Dev.*, 1984, **28**(3), 322–333.